

Pediatric Neurocutaneous Syndromes with Cerebellar Involvement



Thangamadhan Bosemani, MD*,
Thierry A.G.M. Huisman, MD, EQNR, FICIS, Andrea Poretti, MD

KEYWORDS

• Neurocutaneous syndromes • Cerebellum • Intracranial • Children • MR imaging

KEY POINTS

- Neurocutaneous syndromes are associated with widespread cerebellar involvement.
- Cerebellar involvement in certain types of neurocutaneous syndromes may cause neurocognitive deficits, in particular with regard to language and visuospatial abilities in children.
- Accurate characterization of cerebellar involvement may help in the diagnosis and influences long-term neurocognitive prognosis of children with neurocutaneous syndromes.
- In neurocutaneous disorder, cerebellar tumors such as medulloblastoma in basal cell nevus syndrome have a significantly different management regime compared with sporadic medulloblastoma.

INTRODUCTION

Neurocutaneous syndromes (NCS) are a group of congenital disorders of histogenesis in which the overall brain structure may be normal but anomalous cells persist and continue to differentiate. NCS primarily involves structures derived from the neuroectoderm and, consequently, typically affect the skin and central and/or peripheral nervous system. Most textbooks and reviews focus on the description of the typical supratentorial findings in NCS, with few focusing on the coexisting infratentorial lesions. Neuroimaging has proven to play a key role in the characterization, definition, and diagnosis of NCS. The cerebellum is, however, involved in various types of NCS and its careful evaluation should be part of every neuroimaging study in children with NCS. Cerebellar involvement may (1) be helpful or needed

for the diagnosis of certain types of NCS and (2) explain the cognitive and behavioral phenotype (eg, impaired visuospatial ability, impaired language, or abnormal social behavior) of children with some NCS.

This article describes various types of NCS with cerebellar involvement. For each disease or syndrome, clinical features, genetic, neuroimaging findings, and the potential role of the cerebellar involvement is discussed.

NEUROFIBROMATOSIS TYPE 1

Neurofibromatosis type 1 (NF1; Online Mendelian Inheritance in Man [OMIM] entry 162200) is the most common NCS with a prevalence of 1 in 2500 to 3000 individuals.¹ It is an autosomal dominant disorder caused by heterozygous mutation in the neurofibromin gene on chromosome 17q11.2.

Disclosure: The author reports no conflicts of interest.

Section of Pediatric Neuroradiology, Division of Pediatric Radiology, Russell H. Morgan Department of Radiology and Radiological Science, The Johns Hopkins University School of Medicine, Baltimore, MD, USA

* Corresponding author. Section of Pediatric Neuroradiology, Division of Pediatric Radiology, Russell H. Morgan Department of Radiology and Radiological Science, Charlotte R. Bloomberg Children's Center, The Johns Hopkins University School of Medicine, Sheikh Zayed Tower, Room 4174, 1800 Orleans Street, Baltimore, MD 21287-0842.

E-mail address: tbosema1@jhmi.edu

Neuroimaging Clin N Am 26 (2016) 417–434
<http://dx.doi.org/10.1016/j.nic.2016.03.008>

1052-5149/16/\$ – see front matter © 2016 Elsevier Inc. All rights reserved.

Descargado para Anonymous User (n/a) en Asturias Ministry of Health de ClinicalKey.es por Elsevier en enero 03, 2025. Para uso personal exclusivamente. No se permiten otros usos sin autorización. Copyright ©2025. Elsevier Inc. Todos los derechos reservados.

Neurofibromin is widely expressed with high levels in the nervous system and acts as a tumor suppressor. Neurofibromin reduces cell growth and proliferation by negative regulation of the cellular proto-oncogene p21RAS and by control of the serine threonine kinase mammalian target of rapamycin (mTOR).² Impaired neurofibromin function predisposes to benign and malignant tumor formation.

The principal clinical manifestations of NF1 involve the skin and the nervous system, but the complications are variable and may involve most of the body systems.³

Neuroimaging abnormalities in NF1 include intracranial neoplasms, parenchymal T2-hyperintense lesions, cerebral vasculopathy, and sphenoid wing dysplasia. Intracranial neoplasms include glioma, cranial nerve schwannoma, and plexiform neurofibroma.⁴ Gliomas generally develop in the optic pathways, brainstem, and, rarely, cerebellum. Optic pathway gliomas are the most

frequent neoplasms seen in about 15% of children with NF1 and are typically low-grade pilocytic astrocytomas. Parenchymal T2-hyperintense lesions, also referred to as unidentified bright objects, can be seen in up to 75% of pediatric patients with NF1 and tend to decrease in prevalence with advancing age (Fig. 1A).⁴ These lesions are not space occupying, do not or very rarely show contrast enhancement, and are typically located in the basal ganglia, internal capsule, brainstem, and cerebellum. Increased apparent diffusion coefficient (ADC) values in unidentified bright objects match the histopathological finding of myelin vacuolation and spongiotic changes attributed to increased water accumulation.⁵

Primary cerebellar tumors are a rare presentation in NF1. In a series of 600 NF1 subjects, only 2 children had low-grade astrocytomas arising primarily from the cerebellar hemisphere (Fig. 1B).⁶ Vinchon and colleagues⁷ showed an overall better outcome for cerebellar gliomas

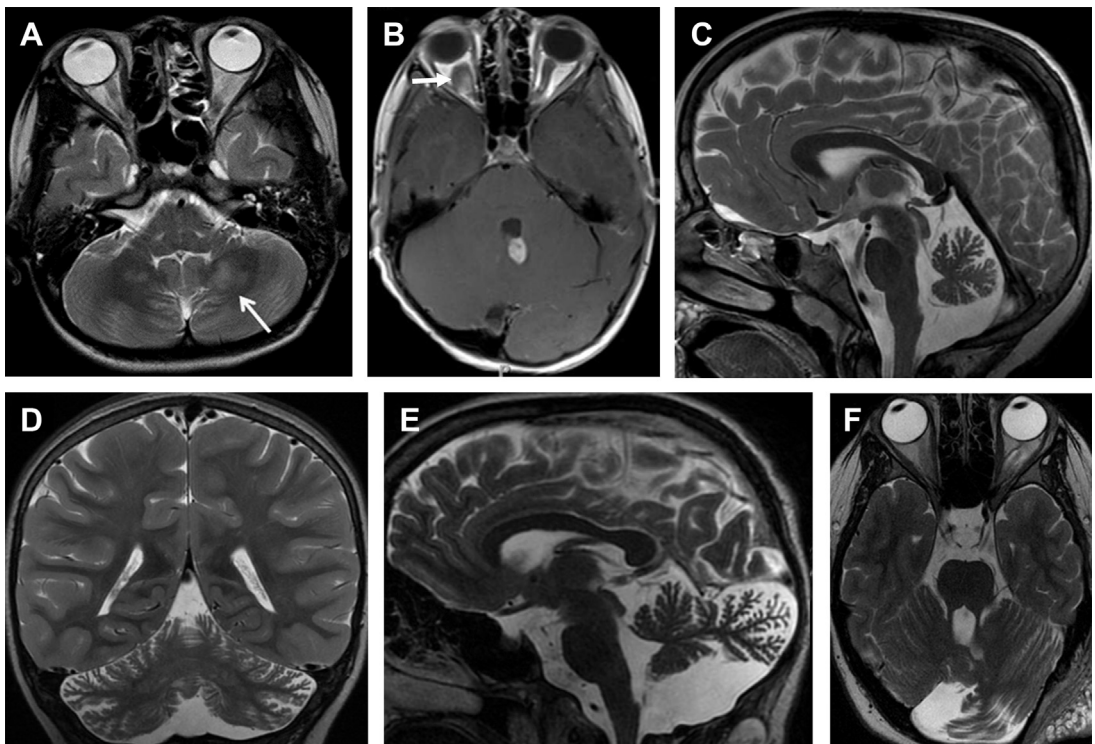


Fig. 1. Neurofibromatosis type 1. (A) Axial T2-weighted image showing cerebellar parenchymal T2-hyperintense lesions (arrow), also referred to as unidentified bright objects. (B) Axial T1 postcontrast image demonstrating an enhancing glioma in the rostral and medial aspect of the cerebellar vermis and optic glioma on the left (arrow). (C) Sagittal and (D) coronal T2-weighted images showing normal size of the cerebellar vermis and hemispheres with stable enlargement of the interfoliar spaces consistent with cerebellar hypoplasia. (E) Sagittal and (F) axial T2-weighted images showing enlargement of the left cerebellar hemisphere. The posteromedial part of the left cerebellar hemisphere is bulky, crosses the midline, and its interfoliar spaces are enlarged, consistent with cerebellar dysmorphia. (From Toelle SP, Poretti A, Weber P, et al. Cerebellar hypoplasia and dysmorphia in neurofibromatosis type 1. *Cerebellum* 2015;14(6):642–9; with permission.)

associated with NF1 compared with sporadic cerebellar gliomas. Cerebellar parenchymal T2-hyperintense lesions can be distinguished from neoplasms based on absence of mass effect and lack of enhancement. Children with cerebellar parenchymal T2-hyperintense lesions showed a lower intelligence quotient and an altered cognitive profile compared with children without the lesions, particularly with regard to language and visuospatial abilities.⁸ Malformative cerebellar abnormalities, including cerebellar hypoplasia and dysmorphia (defined as enlargement of a cerebellar hemisphere with widening of the interfoliar spaces of its posterior part, which is bulky and crosses the midline), are a rare but most likely an underestimated cerebellar manifestation of NF1 (Fig. 1C–F).⁹

TUBEROUS SCLEROSIS COMPLEX

Tuberous sclerosis complex (TSC) is caused by either *TSC1* (OMIM 191100) or *TSC2* (OMIM 613254). It is an autosomal dominant NCS characterized by hamartomas in several organs, including the skin, brain, heart, eyes, kidney, lung, and liver.¹⁰ TSC is due to an inactivating mutation in 1 of the 2 genes, *TSC1* (on chromosome 9q34) encoding hamartin or *TSC2* (on chromosome 16p13.3) encoding tuberin.¹⁰ Hamartin and tuberin work together to inhibit the mTOR pathway that stimulates protein translation, cell growth, and proliferation. Mutations of hamartin or tuberin in TSC cause hyperactivation of the downstream mTOR pathway, which leads to disorganized cellular overgrowth, abnormal differentiation, increased protein translation, and the formation of tumors. Estimated prevalence of TSC is 1 in 6000 to 7000 newborns.

The identification of either a *TSC1* or *TSC2* pathogenic mutation in DNA from normal tissue is sufficient to make a definite diagnosis of TSC.¹¹ Between 10% and 25% of TSC patients have no mutation identified by conventional genetic testing and a normal result does not exclude TSC or have any effect on the use of clinical diagnostic criteria to diagnose TSC.¹¹

Clinical features of TSC most commonly involve the brain (seizures, including infantile spasms, intellectual disability, autism, and self-injurious or aggressive behavior), skin (hypomelanotic macules, angiofibromas, ungula fibromas, shagreen patch, and confetti skin lesions), kidneys (angiomyolipomas and multiple renal cysts), heart (cardiac rhabdomyomas), eyes (multiple retinal hamartomas), and lungs (lymphangioleiomyomatosis in female patients). The 2012 International TSC Consensus Conference updated diagnostic

clinical criteria now include 11 major features and 6 minor features. The 2012 consensus is based on definite (2 major features or 1 major feature with ≥ 2 minor features) or possible (either 1 major feature or ≥ 2 minor features) diagnosis.¹¹ Interestingly, some neurologic symptoms such as seizures and intellectual disability are not part of the diagnostic criteria. Three major diagnostic criteria are based on neuroimaging studies (cortical dysplasias, including tubers and cerebral white matter radial migration lines [RMLs], subependymal nodules, and subependymal giant cell astrocytoma). This means that the diagnosis can be made by brain MR imaging alone.

The neuroimaging manifestations of TSC include cortical tubers, subependymal nodules, subependymal giant cell astrocytomas, and white matter RMLs.⁴ White matter RMLs are the most frequent neuroimaging finding and are strongly associated with age of seizure onset, intelligence outcomes, and level of autistic features.¹² RMLs represent residual or altered heterotopic glial cells and neurons along the course of glial neuronal migration. Cortical tubers observed in approximately 90% of TSC patients are a type of focal cortical dysplasia and may occur in the cerebellum. The pathologic and clinical overlap between cortical tuber as a major feature and RML as a minor feature in the 1998 diagnostic criteria were replaced with a single major feature, cortical dysplasia, in the new 2012 classification.¹¹

Cerebellar tubers are present in 24% to 36% of TSC patients and have a different imaging pattern compared with cerebral tubers.^{13,14} Cerebellar cortical tubers differ from the supratentorial tubers in their imaging features. They are triangular with a broad base towards the cerebellar cortex. The shape results from the differing neuronal migration within the cerebellum compared with the cerebrum. Cerebellar tubers are T1-hypointense, and T2-hyperintense (Fig. 2A). Contrast enhancement with a striated or zebra-like pattern (Fig. 2B) and calcification (Fig. 2C) may be seen.^{13,15} Cerebellar tubers were demonstrated to increase in size, enhancement, or calcification, within the first 8 years of life (Fig. 2D).¹³ Elevated ADC values in cerebellar tubers have been attributed to gliosis and hypomyelination.^{13,15} An increasing number of cerebellar tubers on MR imaging has been correlated with the severity of autistic spectrum disorder.¹⁶ In addition, reduced cerebellar volume has been observed in TSC patients, particularly patients with *TSC2* mutations and a more severe phenotype.¹⁷ Evidence of the role of cerebellar involvement in cognition and behavior in TSC was provided by animal studies. In a *Tsc1* mouse model, Tsai and colleagues¹⁸ showed a decrease

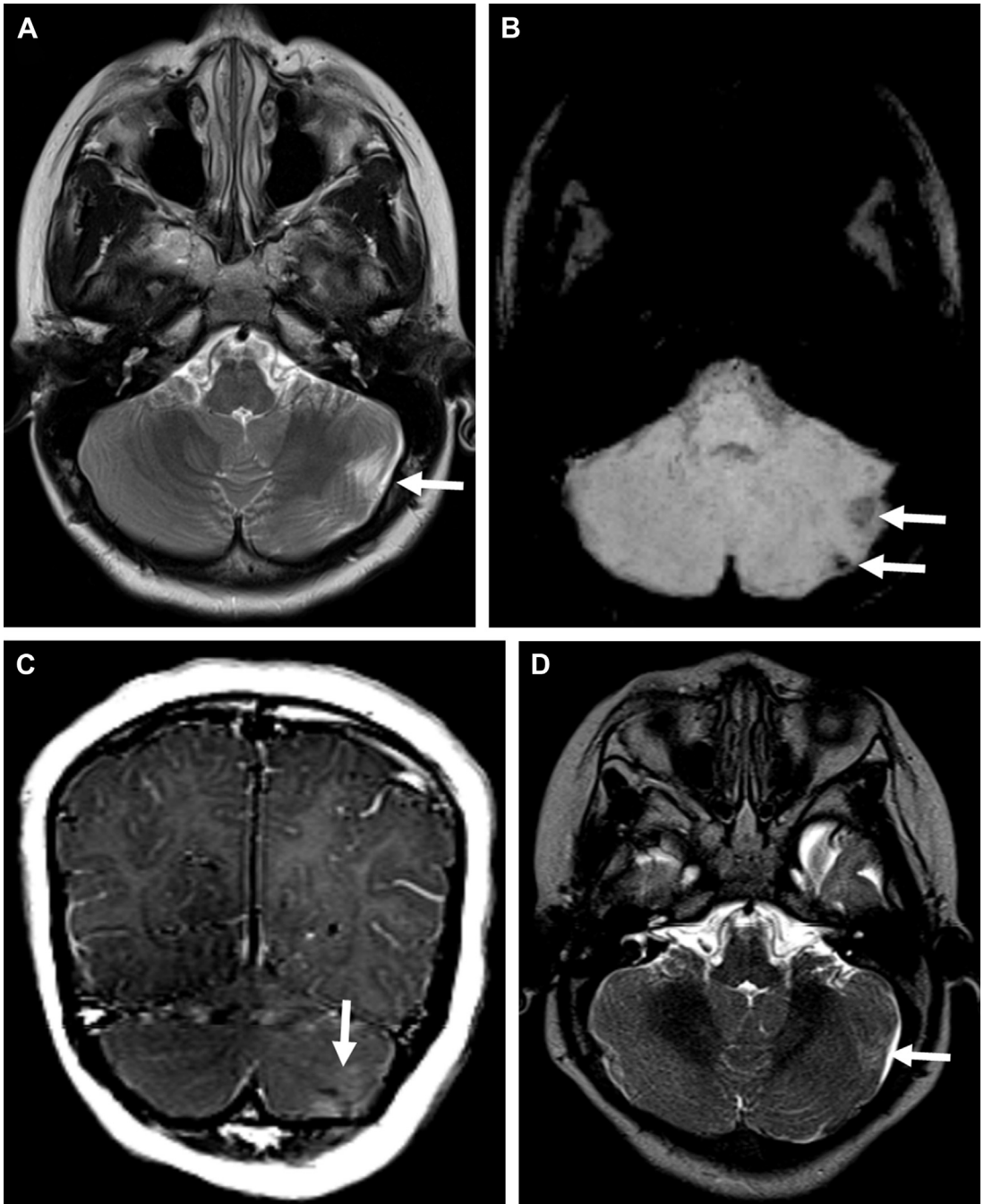


Fig. 2. 5-year-old girl with TSC. (A) Axial T2-weighted image showing a wedge-shaped hyperintense lesion on the left consistent with a cerebellar tuber (arrow). (B) Axial susceptibility-weighted image (SWI) demonstrates hypointensity within the tuber (arrows), suggesting calcification. (C) Coronal T1 postcontrast image showing striated or zebra-like pattern of enhancement (arrow). (D) Axial T2-weighted image at 10-months of age shows a subtle T2 bright cerebellar tuber on the left (arrow) with interval significant increase in dimension at 5-years of age.

in the number of Purkinje cells compared with control. This is the most likely explanation for smaller cerebellar volume in TSC patients. In addition, mutated mice showed an autistic-like behavior as seen in TSC patients.

STURGE-WEBER SYNDROME

Sturge-Weber syndrome (SWS; OMIM 185300) is a sporadic NCS characterized by a facial cutaneous capillary malformation (port-wine stain) in

the ophthalmic distribution of the trigeminal nerve, ipsilateral vascular glaucoma, vascular malformation of the choroid, and a concomitant vascular malformation of the brain and meninges (leptomeningeal angioma).¹⁹ The estimated prevalence of SWS ranges between 1 in 20,000 to 50,000 live births. Specific somatic mosaic activating mutation in *GNAQ* is associated with both SWS and nonsyndromic port-wine stains.²⁰ It is hypothesized that *GNAQ* mutation causes dysregulation of vascular endothelin that may result in malformed, progressively dilated, and abnormally innervated blood vessels.²⁰ Pathophysiological mechanism in SWS can be explained by venous dysplasia producing focal venous hypertension and resultant tissue hypertrophy.²¹ The absence of a mature venous system is initially compensated by the persistence and enlargement of the primitive primordial cerebral venous system. This primitive venous system becomes progressively insufficient with the rapid brain development resulting in intraparenchymal venous hypertension, venous ischemia, tissue injury, and atrophy. Compensatory collateral venous circulatory pathways (eg, dilated intramedullary veins) draining into the deep venous system partially compensate for the venous insufficiency.²² The clinical course of SWS is variable but typically includes seizures, hemiparesis, headache, stroke-like episodes, developmental delay, and visual field defects.²³

Typical neuroimaging findings in SWS include a prominent leptomeningeal angiomatosis (especially well seen on contrast-enhanced T1-weighted and FLAIR images),²⁴ dilated medullary veins, enlargement of the ipsilateral choroid plexus, and underlying slowly progressive cortical or subcortical atrophy. The occipital lobes are primarily affected; in severe cases the central zone, as well as frontal lobes, may also be involved. Rare cases of bilateral involvement have been recorded. Susceptibility-weighted imaging (SWI) is an advanced MR imaging technique that can detect deoxygenated blood in small veins without contrast administration. SWI can detect dilation of transmedullary veins secondary to venous hypertension.²⁵ In addition, progressive cortical calcifications secondary to long-standing venous hypertension or ischemia is easily identified by the T2* blooming artifacts on SWI.

Cerebellar involvement in SWS is rare and includes leptomeningeal enhancement (Fig. 3A), atrophy, and developmental venous anomaly (Fig. 3B–D). ADC-values of the cerebellar white matter remote from the location of the leptomeningeal angioma may be increased.²⁶

PHACE SYNDROME

PHACE syndrome (OMIM 606519) is an NCS characterized by posterior fossa malformation, infantile hemangioma (IH), arterial anomalies, coarctation of the aorta, eye abnormalities, and ventral developmental defects, specifically sternal defects, and/or supraumbilical raphe. The cause and pathogenesis of PHACE is unknown and its diagnosis is based on the presence of a characteristic hemangioma and other major or minor clinical or imaging criteria.²⁷

Isolated IH are subtle or absent at birth, usually becoming more evident within the first days to weeks of life. IH associated with PHACE tend to be large (>5 cm in diameter), telangiectatic in appearance, and typically segmental in distribution in the face.²⁷ Most patients have a normal neurologic examination in infancy but may develop focal seizures, developmental delay, and recurrent headaches.²⁷ Early neurologic findings are typically related to structural brain anomalies.

The presence of a segmental cervicofacial IH should prompt neuroimaging to evaluate for the presence of intracranial abnormalities that may be related to PHACE. Hence, neuroimaging plays a key role in establishing the diagnosis. Intracranial anomalies (cerebrovascular and posterior fossa) are the most common extracutaneous feature of PHACE and are typically ipsilateral to the IH.^{28,29} Intracranial and cervical arteriopathy diagnosed by MR angiography can be categorized as dysgenesis, narrowing, nonvisualization, persistent embryonic carotid-vertebasilar arterial connections, and abnormalities in arterial course and/or origin.²⁸ Arterial dysgenesis is the most common vascular manifestation and is characterized by eccentric outpouching, fusiform enlargement, or aneurysm formation.²⁸ Arteriopathy is more common in the anterior circulation (internal carotid artery) than in the posterior circulation. Perinatal arterial ischemic stroke may be seen. Supratentorial brain abnormalities associated with PHACE include callosal dysgenesis, hemispheric hypoplasia, subependymal heterotopia, polymicrogyria, and extra-axial hemangiomas.³⁰ Posterior fossa anomalies are the most commonly reported brain anomalies in PHACE.^{27,28,30} The typical posterior fossa anomaly is unilateral cerebellar hypoplasia (Fig. 4) with or without involvement of the vermis; whereas a Dandy-Walker malformation (DWM) is less common.²⁸

VON HIPPEL-LINDAU DISEASE

von Hippel-Lindau (VHL) disease (OMIM 193300) is an autosomal dominant NCS characterized by

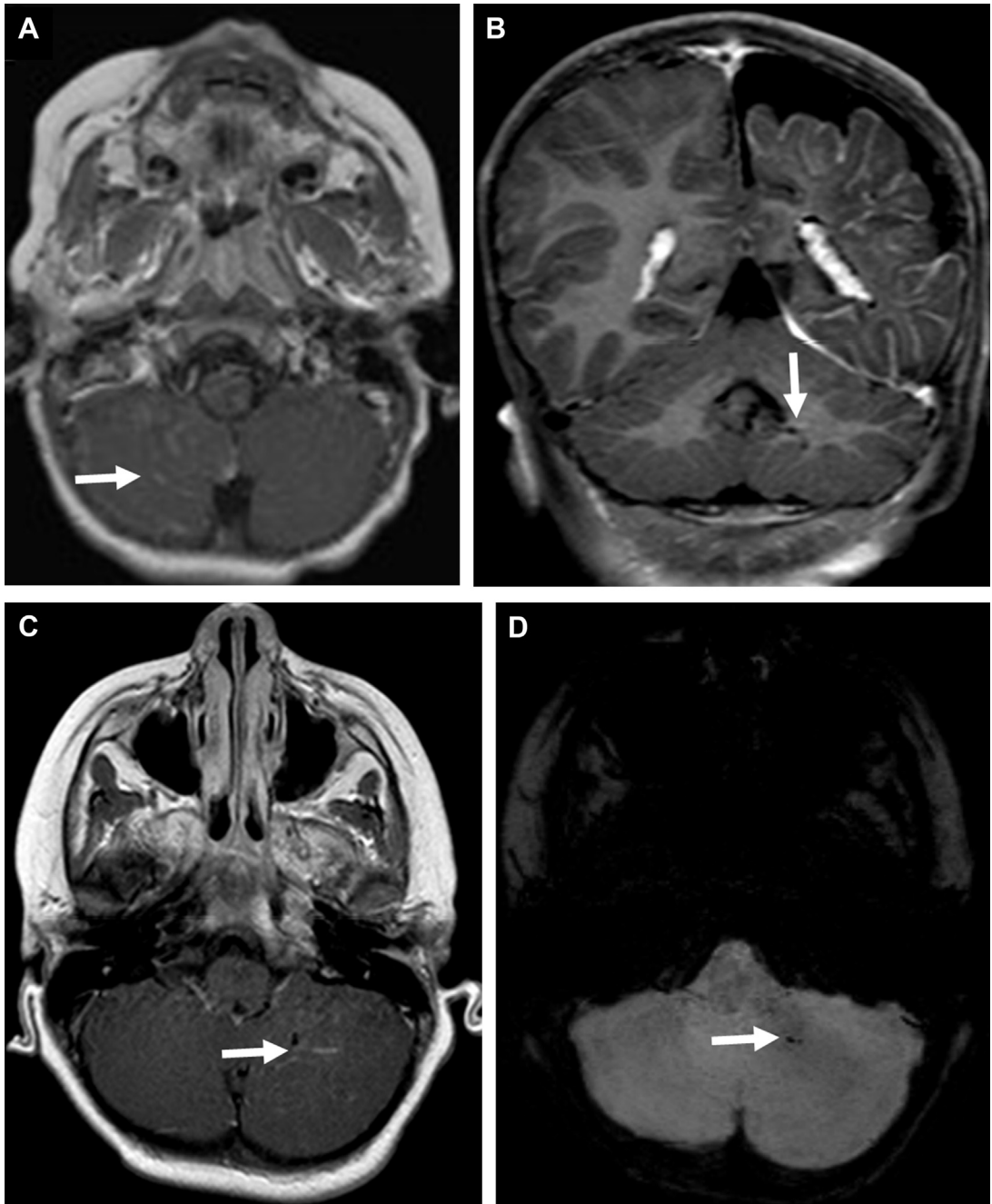


Fig. 3. SWS. (A) Axial T1 postcontrast image showing an enhancing leptomenigeal angioma within the cerebellar fissures on the right (*arrow*). (B) Coronal (*arrow*) and (C) axial T1 postcontrast image showing developmental venous anomaly (DVA) in the left cerebellar hemisphere (*arrow*) and atrophy in the left cerebrum. (D) Axial SWI image showing hypointense signal in the left cerebellar hemisphere DVA (*arrow*). (From [A] Arulrajah S, Ertan G, M Comi A, et al. MR imaging with diffusion-weighted imaging in children and young adults with simultaneous supra- and infratentorial manifestations of Sturge-Weber syndrome. *J Neuroradiol* 2010;37:51–9; with permission.)

various benign and malignant tumors of the central nervous system (CNS), kidneys, adrenal glands, inner ear, and reproductive adnexal organs such as retinal, cerebellar, and spinal

hemangioblastoma and endolymphatic sac tumor. VHL results from a germline mutation in the *VHL* tumor suppressor gene on chromosome 3p25.3, which inactivates a *VHL* allele, with the carriers

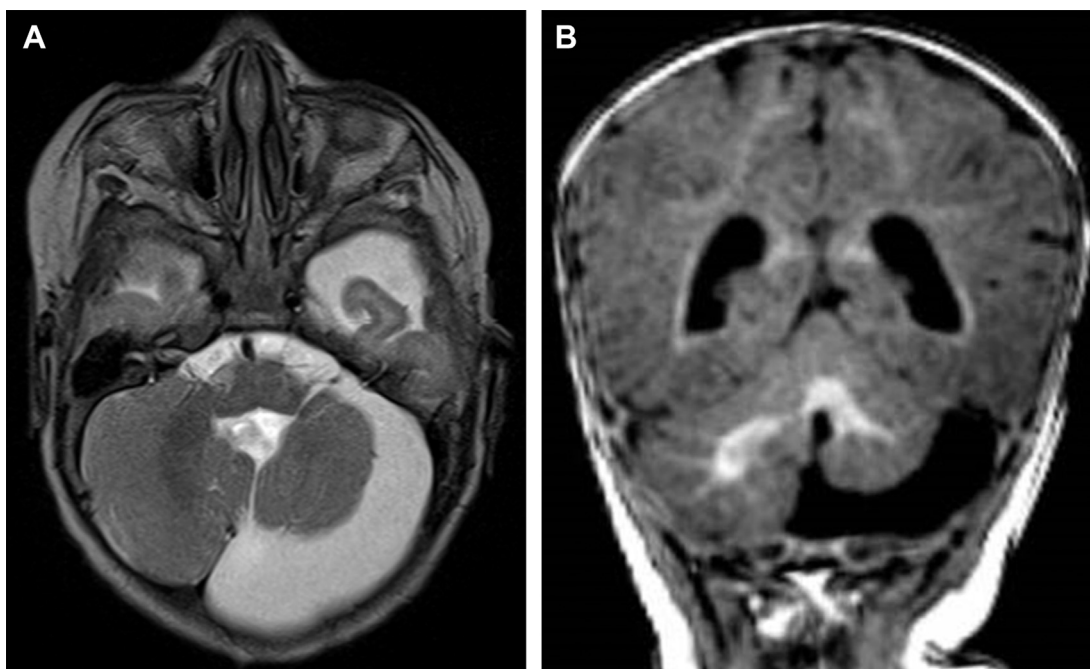


Fig. 4. 4-month-old girl with PHACE syndrome. (A) Axial T2 and (B) coronal T1-weighted images showing unilateral cerebellar hypoplasia with volume loss in the left cerebellar hemisphere and vermis with a normal sized posterior fossa and a prominent extra-axial CSF space subjacent to it.

of this mutation being subject to a second inactivating event (2-hit hypothesis).³¹ This mutation results in complete functional loss of the tumor suppressor and, therefore, overexpression of proteins that mediate angiogenesis. The estimated incidence of VHL is about 1 in 36,000 live births.⁴ Outside the CNS, multisystem visceral involvement includes renal cysts, renal cell carcinomas, pancreatic cysts, and pheochromocytomas. CNS hemangioblastoma is observed in 65% of patients with VHL and is a defining feature in VHL.³²

The cerebellum is the most common location (about 65%) for CNS hemangioblastomas. They are highly vascular benign World Health Organization (WHO) grade 1 tumors that show solid enhancement, appear pial-based, and are, therefore, peripherally located in the cerebellum (Fig. 5). When the tumors enlarge, they appear cystic with an enhancing mural nodule and the natural history of progression shows a faster rate of cystic expansion than growth of the causative solid tumor, eventually resulting in pressure effect and clinical symptoms.³³ Hemangioblastomas are T1-isointense and T2-hyperintense. Heterogeneous T2 signal may be seen in the presence of intralesional hemorrhage. Mural nodules are well demarcated and show homogenous enhancement. If present, flow voids appear T2 hypointense

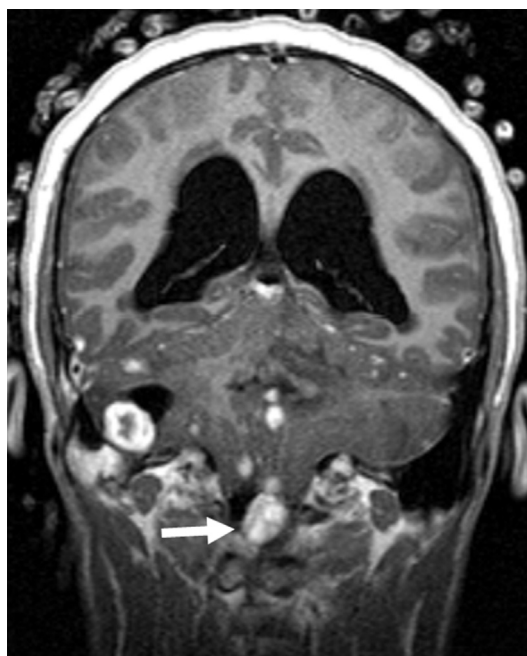


Fig. 5. 16-year-old boy with VHL disease. Coronal T1 postcontrast image demonstrates numerous hemangioblastomas within the cerebellum and in the cervicomedullary junction (arrow).

with superficial heterogeneous enhancement. Peritumoral vasogenic edema is typically mild. In VHL, multiple lesions may occur simultaneously. Additional lesions may be present along the spinal cord. Imaging of the entire neural axis is consequently advised. The lesion may mimic a pilocytic astrocytoma. The clinical findings usually allow differentiation. In addition, hemangioblastomas are typically characterized by the prominent vascular signal voids. Finally, hemangioblastomas may hemorrhage into the subarachnoid space with resultant hemosiderosis due to their high vascular nature and close proximity to the subarachnoid space. Endolymphatic sac tumors are, with a prevalence of up to 16%, a component of VHL disease. Contrast-enhanced MR imaging of the petrous bone must be part of annual surveillance.³⁴

Affected children may present with a history of minor neurologic symptoms, such as occipital or frontal headaches or imbalance. Significant neurologic deficit may result from development of obstructive hydrocephalus, tonsillar herniation, and brainstem compression, requiring immediate neurosurgical intervention.³⁵

NEUROCUTANEOUS MELANOSIS

Neurocutaneous melanosis (NCM; OMIM 249400) is a rare NCS characterized by congenital melanocytic nevi (CMN) associated with CNS involvement.³⁶ CMN can be single or multiple and are present at birth or arise within the first few weeks of life. It has recently been found to be caused by mosaicism for heterozygous somatic mutations in the *NRAS* codon 61 of a progenitor cell within the neuroectoderm.³⁷ NCM is characterized by excessive proliferation of melanocytes in the leptomeninges and brain parenchyma, and is considered an embryologic abnormality of the developing neuroectoderm. MR imaging of the entire neural axis is the modality of choice in children with 2 or more CMN at birth, and performed in the first year of life (ideally within the first 6 months due to progressing myelination, which may obscure the signal of melanin).³⁶

Seizures represent the most common initial neurologic symptom in children.³⁸ Neurodevelopmental delay and increasing intracranial pressure from hydrocephalus are other neurologic symptoms in NCM. Progressive leptomeningeal melanocytosis and/or melanoma of the brain and spine are associated with a poor prognosis. Proliferating leptomeningeal deposits are associated with communicating hydrocephalus and/or increasing intracranial pressure.

The most common neuroimaging abnormality on MR imaging is isolated intraparenchymal

melanosis (foci of melanin-containing cells in the brain parenchyma), which was previously considered to be secondary only to overlying invasive leptomeningeal disease.³⁶ The typical location for melanin deposition with T1-hyperintensity and/or T2 hypointensity is in the anterior regions of the temporal lobes (amygdala), cerebellum, pons, and leptomeningeal surface.³⁸ In addition to T1-hyperintensity (melanin) on the precontrast images, diffuse nodular enhancement may be present postcontrast with progressive leptomeningeal melanocytosis. Diffuse leptomeningeal melanoma may develop and is biopsy proven.

Intraparenchymal melanosis with T1-hyperintense lesions may affect the cerebellum (Fig. 6A). Cerebellar hypoplasia may be associated with NCM (Fig. 6B).

GÓMEZ-LÓPEZ-HERNÁNDEZ SYNDROME

Gómez-López-Hernández (GLH) syndrome (OMIM 601853) also known as cerebello-trigeminal-dermal dysplasia is a rare NCS comprising the triad of rhombencephalosynapsis (RS) (Fig. 7A, B), parietal alopecia (Fig. 7C), and trigeminal anesthesia.³⁹ The cause remains unknown. No chromosomal abnormalities have been reported to date. The clinical signs of GLH (alopecia, trigeminal anesthesia, ataxia, and head stereotypies) can be very mild and easily missed.³⁹ In GLH, there is a broad range of cognitive impairment but cognition can even be normal.³⁹

Neuroimaging plays a key role in establishing RS, which is a key feature of GLH and, hence, is needed for the diagnosis of GLH. RS is characterized by dorsal continuity of the cerebellar hemispheres, agenesis, or hypogenesis of the vermis, and fusion of the dentate nuclei and superior cerebellar peduncles.³⁹ Recently, the absence of trigeminal nerves and foramina rotunda bilaterally has been shown in GLH, suggesting a possible structural basis for trigeminal anesthesia.⁴⁰

ENCEPHALOCRANIOCUTANEOUS LIPOMATOSIS

Encephalocraniocutaneous lipomatosis (ECCL; OMIM 613001) is a sporadic NCS characterized by ocular anomalies, skin lesions, and CNS anomalies.⁴¹ The CNS anomalies in ECCL are most likely caused by a mesenchymal and neural crest defect affecting the tissue surrounding the brain and the vessels.⁴¹

Typical findings include eye anomalies (mainly choristomas) and skin lesions (nonscarring alopecia, nevus psiloliparus, subcutaneous fatty masses, nodular skin tags, or aplastic scalp

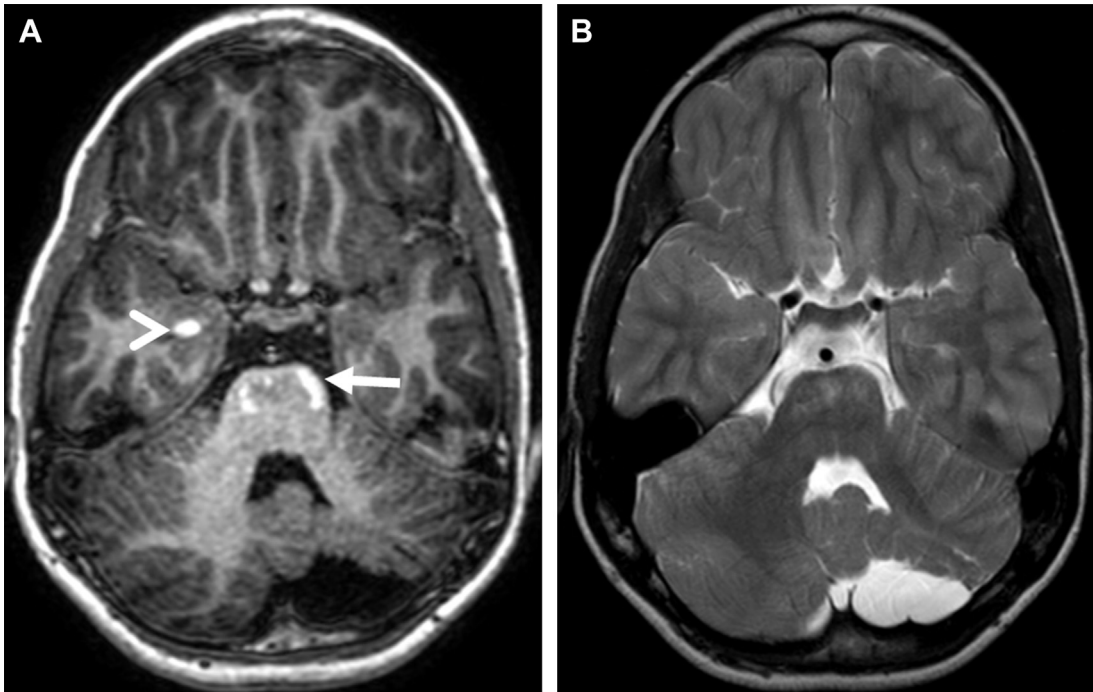


Fig. 6. NCM. (A) Axial T1-weighted image demonstrates hyperintense signal in the anterior aspect of the pons (*arrow*) and right mesial temporal lobe (*arrowhead*) consistent with NCM. Cerebellar hypoplasia is shown on the left. (B) Axial T2-weighted image showing cerebellar hypoplasia on the left with volume loss in a normalized posterior fossa.

defects), which may be unilateral or bilateral.⁴² Children with ECCL may present with developmental delay, intellectual disability, and/or seizures. Neurodevelopmental delay is not related to the severity of neuroimaging findings.

Neuroimaging plays an important role in identifying the CNS anomalies. Posterior fossa involvement in ECCL may include DWM, cerebellar

hypoplasia (**Fig. 8A, B**), arachnoid cysts, and mega cisterna magna. The common CNS anomalies include (1) intracranial lipomas (predominantly cerebello-pontine angle in location) (**Fig. 8C**), (2) spinal lipomas (**Fig. 8D**), (3) arachnoid cysts, (4) intracranial vessel anomalies, (5) unilateral ventriculomegaly, and (6) widening of subarachnoid spaces. Lipomas may be characterized by the

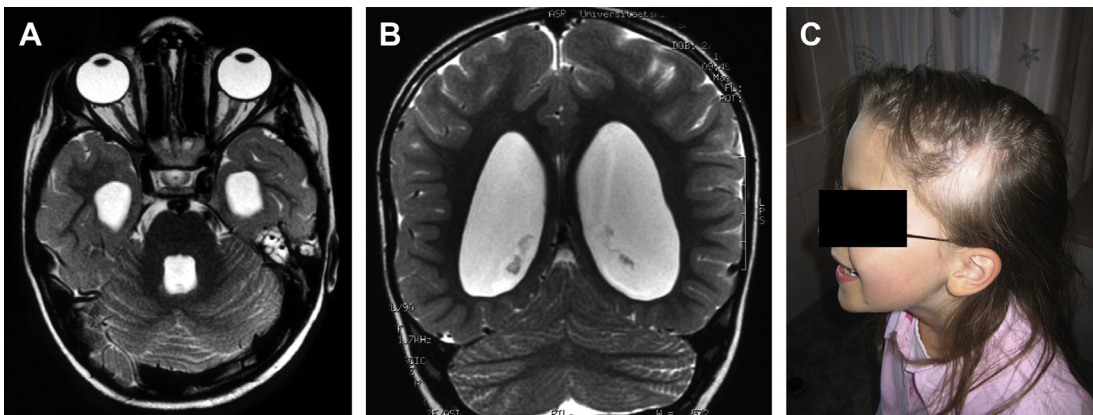


Fig. 7. GLH syndrome. (A) Axial and (B) coronal T2-weighted images showing RS with keyhole appearance of fourth ventricle, fusion of the cerebellar hemispheres without an intervening vermis, as well as fusion of the dentate nuclei and superior cerebellar peduncles. (C) 10-year-old girl with GLH syndrome showing alopecia in the left scalp.

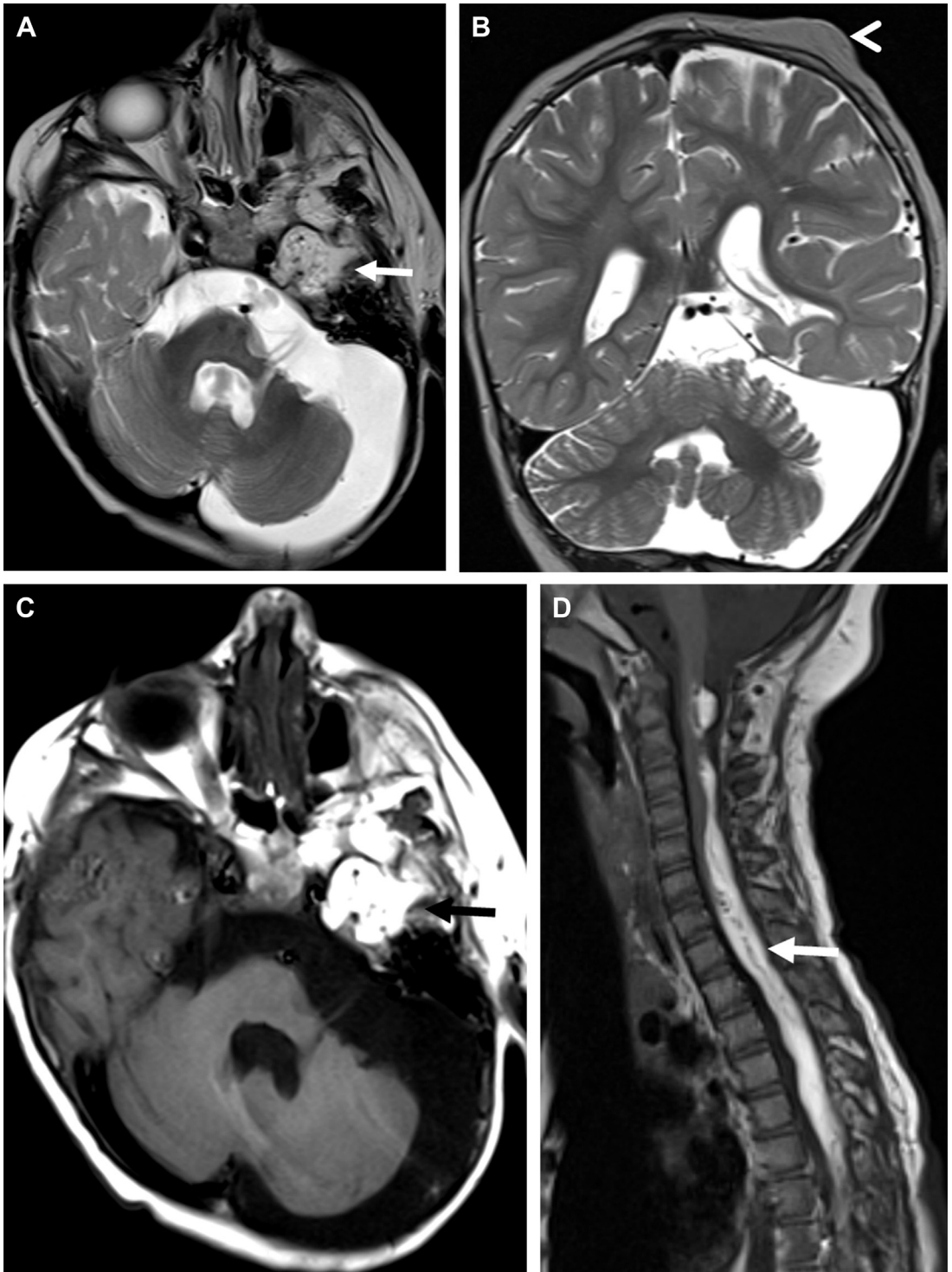


Fig. 8. ECCL. Axial and coronal T2-weighted images showing left cerebellar hypoplasia with prominent CSF space subjacent to left cerebellar hemisphere. (A) Intracranial lipoma infiltrating the left petrous temporal bone (*arrow*) and (B) scalp lesion (*arrowhead*). (C) Axial T1-weighted image demonstrates left cerebellar hypoplasia and T1 bright lipoma (*black arrow*) infiltrating the left petrous temporal bone. (D) Sagittal T1-weighted image of the cervical spine showing epidural location of intraspinal lipoma (*arrow*).

presence and suppression of fat signal on T1-weighted with and without fat suppression, respectively.

OCULOCEREBRO CUTANEOUS SYNDROME

Oculocerebrocutaneous syndrome (OCCS; OMIM 164180), also known as Delleman Oorthuys syndrome is a rare sporadic NCS characterized by the triad of eye, brain, and skin malformations.⁴³ There is a male preponderance. The cause is unknown.

The typical eye findings include orbital cyst, microphthalmia or anophthalmia, and eyelid coloboma. Cutaneous lesions described in OCCS are skin appendages, focal dermal hypoplasia or aplasia, punch-like defects, and crescent-shaped hypoplasia.⁴³

Neuroimaging demonstrates a forebrain malformation consisting of frontal predominant polymicrogyria; periventricular nodular heterotopia, located beneath the polymicrogyria; complete or partial agenesis of the corpus callosum, sometimes associated with interhemispheric cysts; and supratentorial ventriculomegaly. Moog and colleagues⁴³ described a novel mid-hindbrain malformation consisting of a giant dysplastic tectum and absent vermis. The midbrain is angled more forward than normal, leading to a short, horizontal aqueduct, enlarging prematurely into the fourth ventricle. The combination of a giant dysplastic tectum and absent vermis is pathognomonic for OCCS (Fig. 9). In addition, the cerebellar hemispheres are hypoplastic with a dysplastic foliar pattern. The absence of the vermis and cerebellar hypoplasia leads to wide communication of the fourth ventricle with a posterior fossa cerebrospinal fluid (CSF) space.

EPIDERMAL NEVUS SYNDROME

Epidermal nevus syndrome (ENS) includes a heterogeneous group of primary sporadic NCS

characterized by the presence of epidermal nevi that follow the lines of Blaschko and are associated with systemic involvement.⁴⁴ ENS are neurocristopathies due to defective neural crest development. The incidence of ENS is unknown.

The principal manifestations of ENS are epilepsy, developmental delay, intellectual disability, and focal motor deficits. Hemimegalencephaly (HME) is the primary cause of epilepsy in all forms of ENS but often is unrecognized.⁴⁴ HME is present in more than 50% of children with ENSs and neurologic symptoms. MR imaging is the neuroimaging tool of choice for evaluation of HME. The typical MR imaging appearance of HME includes a moderate to marked enlargement of the affected cerebral hemisphere with midline shift, a thickened cortex with broad gyri, shallow sulci and blurring of the cortical-white matter junction, cortical thickening, an increased volume and T2-hyperintense signal of the white matter, and enlarged lateral ventricle with straightening of the frontal horn and/or unilateral colpocephaly.⁴⁵ Ipsilateral enlargement of the cerebellum and brain stem is referred to as total HME (Fig. 10) and has been reported in several cases of ENS.⁴⁶

PTEN HAMARTOMA TUMOR SYNDROME

PTEN hamartoma tumor syndrome (PHTS) is an autosomal dominant cancer-predisposition syndrome caused by mutations in the tumor suppressor gene *PTEN* on chromosome 10q23.31.⁴⁷ PHTS includes Cowden syndrome, Bannayan-Riley-Ruvalcaba syndrome, Proteus syndrome, and Proteus-like syndrome. These allelic disorders are associated with unregulated cellular proliferation leading to the formation of hamartomas. Children and adults with PHTS are at increased risk for benign and malignant tumors of various organs, including the thyroid, breast, endometrium, skin, kidneys, CNS, and gastrointestinal tract.

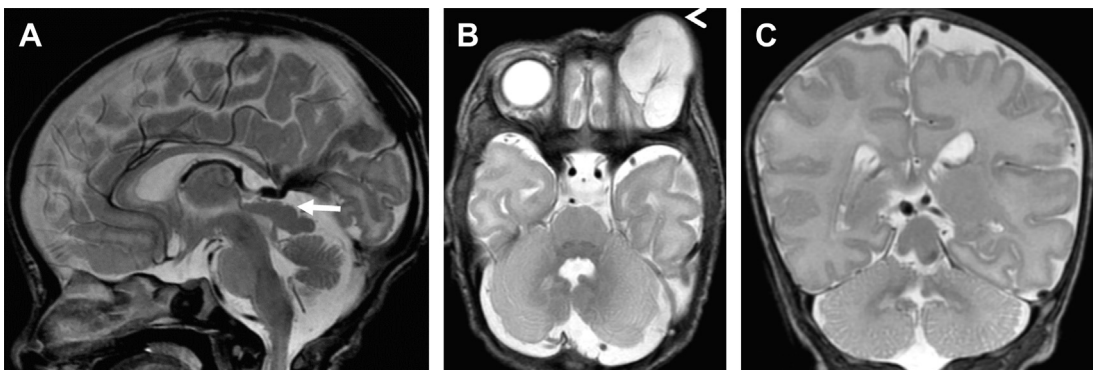


Fig. 9. OCCS. Sagittal, axial, and coronal T2-weighted images showing (A) giant dysplastic tectum (arrow), (B) left orbital cyst (arrowhead), and (C) absent vermis.

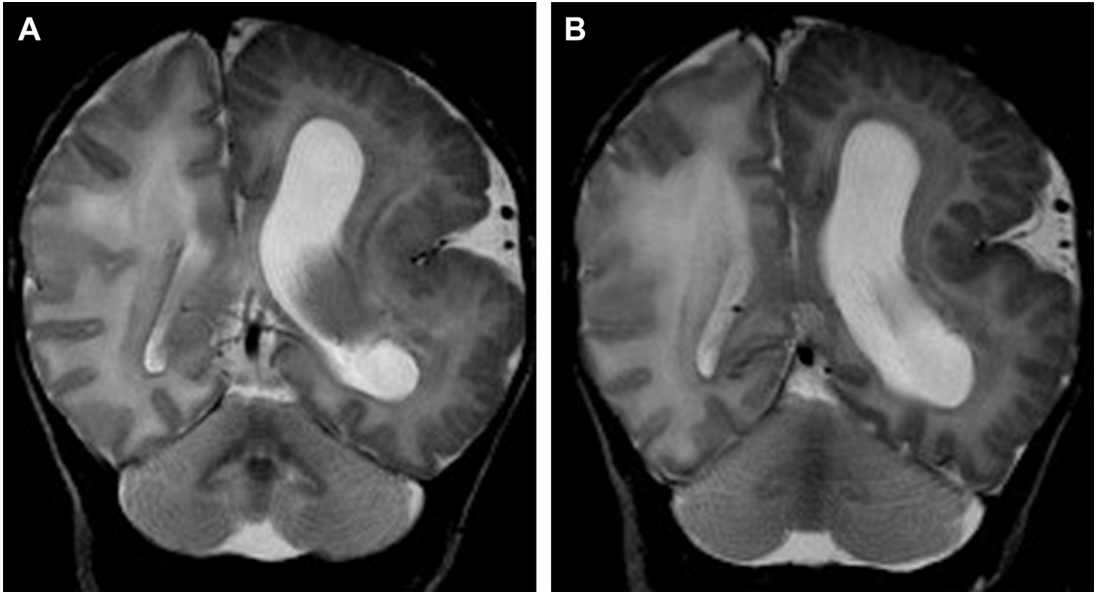


Fig. 10. ENS. (A, B) Coronal T2-weighted images demonstrate total HME with enlargement of the cerebral hemisphere and ipsilateral cerebellar hemisphere. The enlarged cerebral hemisphere shows a thickened cortex with broad gyri, shallow sulci with blurring of the cortical-white matter junction, and T2-hyperintense signal of the white matter.

Although most tumors occur only in adulthood, tumors have been reported in children.⁴⁷

Macrocephaly is a consistent finding. Intellectual and developmental disability is a common finding in children with PTEN mutations. A child with developmental concerns, who exhibits any finding of PHTS (eg, macrocephaly, pigmented penile macules, lipomas, vascular malformations) at any age should be suspected of having PHTS.⁴⁷

Lhermitte-Duclos disease (LDD) is a rare overgrowth of hamartoma arising from the cerebellar cortex characterized by abnormal ganglion cells, absence of Purkinje cells, and hypertrophy of granular cell layer.⁴⁸ LDD is commonly sporadic but can also be familial if associated with Cowden syndrome.⁴⁹ LDD typically manifests during the third and fourth decades of life but may also present in childhood. Clinical manifestations of a posterior fossa mass include headaches, cerebellar ataxia, and perturbed vision.

Neuroimaging pattern of multifocal static white matter abnormalities and dilated perivascular spaces should suggest the possibility of a PHTS in a child with macrocephaly and developmental delay and/or autism spectrum disorder.^{50,51}

Typical MR imaging findings of LDD are a discrete stable, nonprogressive cerebellar mass lesion with a striated corduroy or tiger-striped folia pattern. The central T2-hyperintense and T1-hypointense regions relative to gray matter

correspond to the unmyelinated white matter, widened granular cell layer, and the inner portions of the dysplastic molecular layer. The outer T1- and T2-isointense to hypointense regions relative to gray matter correspond to the outer molecular layer and leptomeninges (Fig. 11).⁵² Expansion of the cortex, infiltration of the brain stem, and a space-occupying mass are typical imaging findings of LDD. LDD typically does not show enhancement postcontrast; however, several exceptional cases have been reported.⁵³

BASAL CELL NEVUS SYNDROME

Basal cell nevus syndrome (BCNS; OMIM 109400), also known as Gorlin-Goltz syndrome, is an autosomal dominant disorder characterized by multiple basal cell carcinomas, jaw cysts, palmar or plantar pits, calcification of the falx cerebri, and spine and rib anomalies.⁵⁴ The estimated prevalence of BCNS is 1 in 56,000 to 256,000.⁵⁵ There is no gender or ethnic predilection. BCNS originates from a heterozygous germline mutation in the Patched homolog 1 is a transmembrane glycoprotein that is encoded by the gene *PTCH1* on chromosome 9q22 to 31 and serves as a tumor suppressor of the sonic Hedgehog signaling pathway.⁵⁵

The clinical hallmarks of the disease include multiple basal cell carcinomas of the skin, medulloblastoma, and odontogenic keratocysts (OKCs)



Fig. 11. LDD. (A) Axial T2- and (B) axial T1 postcontrast images showing a left cerebellar hemisphere mass with a striated corduroy or tiger-stripped folia pattern. Striated pattern consists of central T2-hyperintense and T1-hypointense regions as well as peripheral T1- and T2-isointense to hypointense regions relative to gray matter. Mass effect on the fourth ventricle and no significant postcontrast enhancement is shown.

of the oral cavity.⁵⁶ Children with BCNS have a predisposition for secondary tumors after exposure to both ionizing and ultraviolet radiation.⁵⁷ Medulloblastoma treatment usually includes radiation therapy to the posterior fossa, and management of OKCs keratocysts may require sequential computed tomography (CT) imaging studies. It is important to make a diagnosis of BCNS as early as possible to avoid unnecessary exposures to ionizing radiation.⁵⁶

OKCs can be seen in the maxilla and mandible of children. Initial diagnosis of OKC is typically made on maxillofacial CT and follow-up examination with MR imaging is recommended due to the sensitivity of BCNS children to ionizing radiation. Osseous bridging of the sella turcica is rare in the general population but represents an important imaging clue for the diagnosis of BCNS. Macrocephaly is often provided as part of the patients clinical history as the indication for brain imaging. Hence, in the context of macrocephaly, it is important to evaluate for ectopic calcifications, bony bridging of the sella, or other clinical features compatible with BCNS.⁵⁶

Medulloblastoma is frequently the first manifestation of BCNS. The median age of presentation in BCNS (2 years) is much earlier

than in the sporadic presentation (6.9 years). Desmoplastic medulloblastoma (DMB) variant and medulloblastoma with extensive nodularity (MBEN) are histologic variants associated with BCNS.^{58,59} DMB is typically more laterally situated within the cerebellar hemispheres and is frequently associated with meningeal enhancement. DMB and MBEN are considered to have favorable prognosis, an important consideration when the diagnosis of BCNS coexists and radiation therapy is omitted.⁵⁶

COCKAYNE SYNDROME

Cockayne syndrome (OMIM 216400) is an autosomal recessive multisystem NCS characterized by developmental delay, microcephaly, severe growth failure, cutaneous photosensitivity, dental decay, and pigmentary retinopathy. Cockayne syndrome is caused by mutations in *ERCC6* (CSB) in 65% of patients and *ERCC8* (CSA) in the remainder.⁶⁰ The CSA and CSB proteins are involved in nucleotide excision repair, which is closely related to the basal transcription machinery and preferentially targets DNA lesions in actively transcribed genes.⁶¹ There is lack of recovery of RNA synthesis in

cultured skin fibroblasts after ultraviolet irradiation, which may explain the cutaneous manifestations.

Cockayne syndrome is a progressive disorder and there is a spectrum of symptom severity. The cardinal neuroimaging features of Cockayne syndrome include cerebral and cerebellar atrophy, calcifications, and white matter anomalies

(**Fig. 12**).⁶¹ Cerebral white matter loss and ventricular dilation are the earliest signs on MR imaging. Calcifications are typically bilateral and symmetric, most frequently seen in the putamen. Progressive cerebellar atrophy is a common feature and contributes to the diagnosis. Dysmetria and action tremor progress over time with progressive cerebellar atrophy.⁶¹

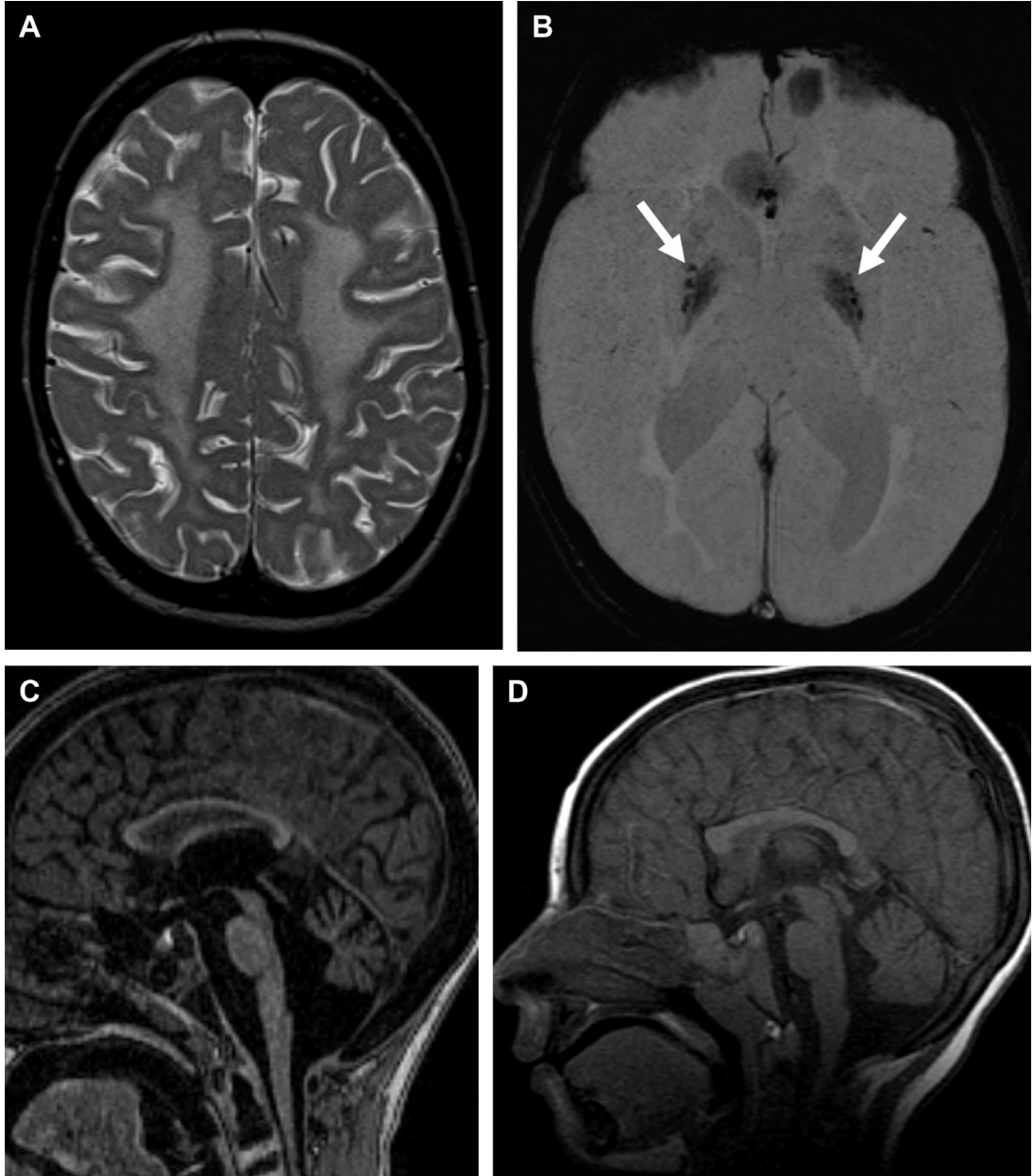


Fig. 12. 9-year-old girl with Cockayne syndrome. (A) Axial T2-weighted image shows confluent abnormal hyperintense signal in the supratentorial white matter. (B) Axial SWI image shows hypointense signal in bilateral globi pallidi (arrows) consistent with calcifications. (C) and (D) Sagittal T1-weighted images at 9-years and 2-years of age, respectively, showing progressive cerebellar atrophy. (From Wagner MW, Poretti A, Wang T, et al. Susceptibility-weighted imaging for calcification in Cockayne syndrome. *J Pediatr* 2014;165(2):416; with permission.)

TRICHOThIODYSTROPHY

Trichothiodystrophy (TTD) is a rare, autosomal recessive NCS, characterized by brittle, sulfur-deficient hair and multisystem abnormalities.⁶² TTD results from defective repair of nucleotide errors in DNA. It is caused by mutations of *XPD*, rarely of *XPB*, *TTDA*, and *TTDN1*; the latter 2 are not associated with photosensitivity.⁶³

Skin findings of photosensitivity and/or ichthyosis were reported in 70% of these patients. Neurologic abnormalities (86%) were frequently reported, manifesting most commonly as developmental delay, intellectual impairment, microcephaly, impaired motor control, or psychomotor retardation.⁶² Neurologic abnormalities seem to be mainly related to impaired development and maturation of the nervous system.⁶⁴

The most common neuroimaging abnormalities are white matter anomalies, cerebellar atrophy, and ventriculomegaly (Fig. 13).⁶²

COSTELLO SYNDROME

Costello syndrome (CoS; OMIM 218040) is an autosomal dominant disorder caused by heterozygous germline mutations in proto-oncogene *HRAS*. Prolonged activation of the *HRAS* protein

results in dysregulation of the Ras/mitogen-activated protein kinase pathway. Ras/mitogen-activated-protein kinase pathway determines cell proliferation and differentiation, and its dysregulation affects cardiac and brain development.⁶⁵

CoS can be diagnosed clinically in the older child with a characteristic facial appearance of curly or fine hair, prominent epicanthal folds, long eyelashes, full nasal tip, fleshy ear lobes, and a wide mouth with full lips.⁶⁵ Infants demonstrate hypotonia, irritability, developmental delay, and nystagmus with delayed visual maturation improving with age. Macrocephaly is a typical finding and likely reflects brain overgrowth.⁶⁶

Disproportionate cerebellar size due to brain overgrowth and a normal-sized posterior fossa results in crowding of the posterior fossa. Gripp and colleagues⁶⁶ showed posterior fossa crowding with cerebellar tonsillar herniation in 96% of subjects and 59% of subjects with serial studies showed progression of posterior fossa crowding. Ventriculomegaly may be seen. Severely affected individuals with cerebellar tonsillar herniation had known complications of hydrocephalus requiring shunt or ventriculostomy, Chiari 1 malformation, and syrinx formation (Fig. 14).⁶⁶ Neurologic symptoms secondary to cerebellar tonsillar herniation

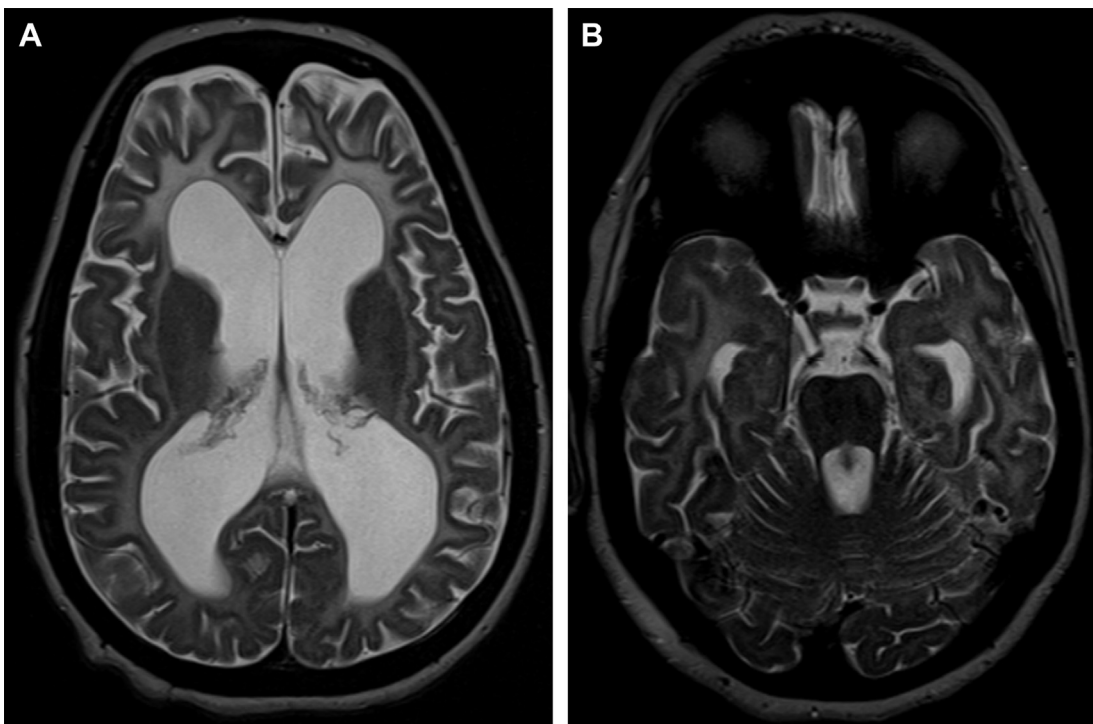


Fig. 13. 14-year-old boy with TTD. (A) and (B) Axial T2-weighted images show diffuse abnormal T2-hyperintense signal of the supratentorial white matter, ventriculomegaly, and cerebellar atrophy.

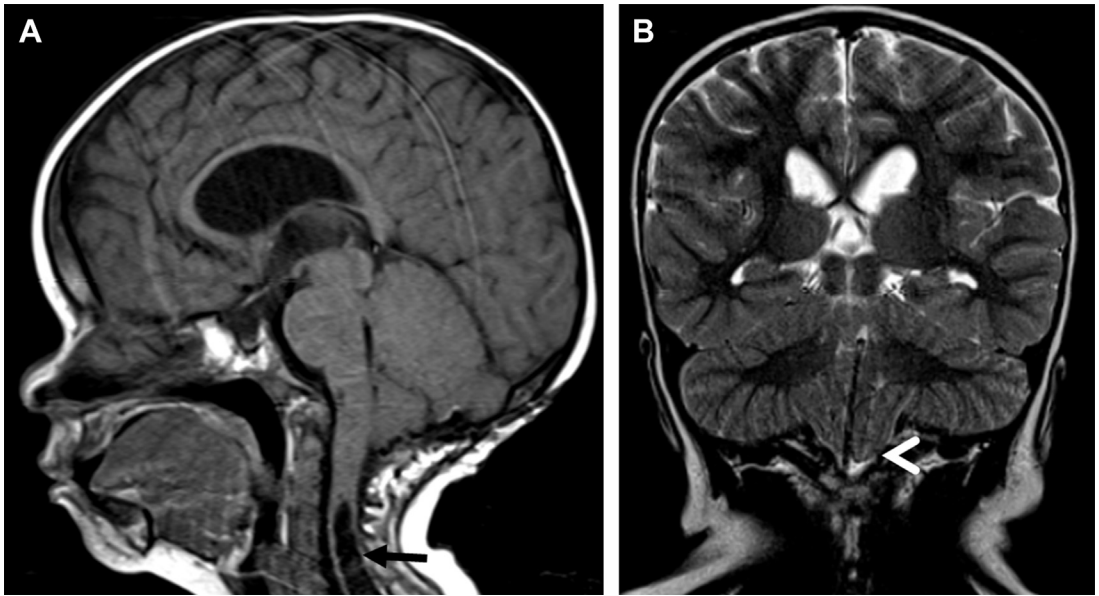


Fig. 14. 6-year-old boy with CoS status post cervicomedullary decompression. (A) Sagittal T1-weighted image shows inferior descent of the cerebellar tonsils, postsurgical changes associated with decompression, and a cervical region syrigo-hydromyelia (arrow). (B) Coronal T2-weighted image shows inferior descent of the cerebellar tonsils (arrowhead).

may be present and require neurosurgical posterior fossa decompression.

SUMMARY

The cerebellum is affected in a wide number of NCS. Neuroimaging plays an important role in the recognition of cerebellar involvement. Accurate recognition and characterization of cerebellar involvement in NCS allows the clinician to: (1) establish the diagnosis, (2) predict the prognosis, (3) support clinical findings/diagnosis, and (4) determine its influence on neurocognitive outcome.

REFERENCES

- Williams VC, Lucas J, Babcock MA, et al. Neurofibromatosis type 1 revisited. *Pediatrics* 2009;123:124–33.
- Ferner RE. The neurofibromatoses. *Pract Neurol* 2010;10:82–93.
- Ferner RE, Gutmann DH. Neurofibromatosis type 1 (NF1): diagnosis and management. *Handb Clin Neurol* 2013;115:939–55.
- Nandigam K, Mechtler LL, Smirniotopoulos JG. Neuroimaging of neurocutaneous diseases. *Neurol Clin* 2014;32:159–92.
- Ertan G, Zan E, Yousem DM, et al. Diffusion tensor imaging of neurofibromatosis bright objects in children with neurofibromatosis type 1. *Neuroradiol J* 2014;27:616–26.
- Pascual-Castroviejo I, Pascual-Pascual SI, Viano J, et al. Posterior fossa tumors in children with neurofibromatosis type 1 (NF1). *Childs Nerv Syst* 2010;26:1599–603.
- Vinchon M, Soto-Ares G, Ruchoux MM, et al. Cerebellar gliomas in children with NF1: pathology and surgery. *Childs Nerv Syst* 2000;16:417–20.
- Piscitelli O, Digilio MC, Capolino R, et al. Neurofibromatosis type 1 and cerebellar T2-hyperintensities: the relationship to cognitive functioning. *Dev Med Child Neurol* 2012;54:49–51.
- Toelle SP, Poretti A, Weber P, et al. Cerebellar hypoplasia and dysmorphism in neurofibromatosis type 1. *Cerebellum* 2015;14(6):642–9.
- Curatolo P, Maria BL. Tuberous sclerosis. *Handb Clin Neurol* 2013;111:323–31.
- Northrup H, Krueger DA. International tuberous sclerosis complex consensus G. Tuberous sclerosis complex diagnostic criteria update: recommendations of the 2012 International Tuberous Sclerosis Complex Consensus Conference. *Pediatr Neurol* 2013;49:243–54.
- van Eeghen AM, Ortiz-Teran L, Johnson J, et al. The neuroanatomical phenotype of tuberous sclerosis complex: focus on radial migration lines. *Neuroradiology* 2013;55:1007–14.
- Daghistani R, Rutka J, Widjaja E. MRI characteristics of cerebellar tubers and their longitudinal changes in children with tuberous sclerosis complex. *Childs Nerv Syst* 2015;31:109–13.

14. Vaughn J, Hagiwara M, Katz J, et al. MRI characterization and longitudinal study of focal cerebellar lesions in a young tuberous sclerosis cohort. *AJNR Am J Neuroradiol* 2013;34:655–9.
15. Ertan G, Arulrajah S, Tekes A, et al. Cerebellar abnormality in children and young adults with tuberous sclerosis complex: MR and diffusion weighted imaging findings. *J Neuroradiol* 2010;37:231–8.
16. Weber AM, Egelhoff JC, McKellop JM, et al. Autism and the cerebellum: evidence from tuberous sclerosis. *J Autism Dev Disord* 2000;30:511–7.
17. Weisenfeld NI, Peters JM, Tsai PT, et al. A magnetic resonance imaging study of cerebellar volume in tuberous sclerosis complex. *Pediatr Neurol* 2013;48:105–10.
18. Tsai PT, Hull C, Chu Y, et al. Autistic-like behaviour and cerebellar dysfunction in Purkinje cell Tsc1 mutant mice. *Nature* 2012;488:647–51.
19. Nabbout R, Juhasz C. Sturge-Weber syndrome. *Handb Clin Neurol* 2013;111:315–21.
20. Shirley MD, Tang H, Gallione CJ, et al. Sturge-Weber syndrome and port-wine stains caused by somatic mutation in GNAQ. *N Engl J Med* 2013;368:1971–9.
21. Parsa CF. Focal venous hypertension as a pathophysiologic mechanism for tissue hypertrophy, port-wine stains, the Sturge-Weber syndrome, and related disorders: proof of concept with novel hypothesis for underlying etiological cause (an American Ophthalmological Society thesis). *Trans Am Ophthalmol Soc* 2013;111:180–215.
22. Vezina G. Neuroimaging of phakomatoses: overview and advances. *Pediatr Radiol* 2015;45(Suppl 3):433–42.
23. Sudarsanam A, Ardern-Holmes SL. Sturge-Weber syndrome: from the past to the present. *Eur J Paediatr Neurol* 2014;18:257–66.
24. Griffiths PD, Coley SC, Romanowski CA, et al. Contrast-enhanced fluid-attenuated inversion recovery imaging for leptomeningeal disease in children. *AJNR Am J Neuroradiol* 2003;24:719–23.
25. Hu J, Yu Y, Juhasz C, et al. MR susceptibility weighted imaging (SWI) complements conventional contrast enhanced T1-MRI in characterizing brain abnormalities of Sturge-Weber Syndrome. *J Magn Reson Imaging* 2008;28:300–7.
26. Arulrajah S, Ertan G, M Comi A, et al. MRI with diffusion-weighted imaging in children and young adults with simultaneous supra- and infratentorial manifestations of Sturge-Weber syndrome. *J Neuroradiol* 2010;37:51–9.
27. Metry D, Heyer G, Hess C, et al. Consensus statement on diagnostic criteria for PHACE syndrome. *Pediatrics* 2009;124:1447–56.
28. Hess CP, Fullerton HJ, Metry DW, et al. Cervical and intracranial arterial anomalies in 70 patients with PHACE syndrome. *AJNR Am J Neuroradiol* 2010;31:1980–6.
29. Bracken J, Robinson I, Snow A, et al. PHACE syndrome: MRI of intracerebral vascular anomalies and clinical findings in a series of 12 patients. *Pediatr Radiol* 2011;41:1129–38.
30. Metry DW, Haggstrom AN, Drolet BA, et al. A prospective study of PHACE syndrome in infantile hemangiomas: demographic features, clinical findings, and complications. *Am J Med Genet A* 2006;140:975–86.
31. Monsalve J, Kapur J, Malkin D, et al. Imaging of cancer predisposition syndromes in children. *Radiographics* 2011;31:263–80.
32. Kanno H, Kuratsu J, Nishikawa R, et al. Clinical features of patients bearing central nervous system hemangioblastoma in von Hippel-Lindau disease. *Acta Neurochir (Wien)* 2013;155:1–7.
33. Lin DD, Barker PB. Neuroimaging of phakomatoses. *Semin Pediatr Neurol* 2006;13:48–62.
34. Bausch B, Wellner U, Peyre M, et al. Characterization of endolymphatic sac tumors and von Hippel-Lindau disease in the International Endolymphatic Sac Tumor Registry. *Head Neck* 2016. [Epub ahead of print].
35. Vortmeyer AO, Falke EA, Glasker S, et al. Nervous system involvement in von Hippel-Lindau disease: pathology and mechanisms. *Acta Neuropathol* 2013;125:333–50.
36. Waelchli R, Aylett SE, Atherton D, et al. Classification of neurological abnormalities in children with congenital melanocytic naevus syndrome identifies MRI as the best predictor of clinical outcome. *Br J Dermatol* 2015;173(3):739–50.
37. Kinsler VA, Thomas AC, Ishida M, et al. Multiple congenital melanocytic nevi and neurocutaneous melanosis are caused by postzygotic mutations in codon 61 of NRAS. *J Invest Dermatol* 2013;133:2229–36.
38. Ramaswamy V, Delaney H, Haque S, et al. Spectrum of central nervous system abnormalities in neurocutaneous melanocytosis. *Dev Med Child Neurol* 2012;54:563–8.
39. Poretti A, Bartholdi D, Gobara S, et al. Gomez-Lopez-Hernandez syndrome: an easily missed diagnosis. *Eur J Med Genet* 2008;51:197–208.
40. Choudhri AF, Patel RM, Wilroy RS, et al. Trigeminal nerve agenesis with absence of foramina rotunda in Gomez-Lopez-Hernandez syndrome. *Am J Med Genet A* 2015;167A:238–42.
41. Moog U, Jones MC, Viskochil DH, et al. Brain anomalies in encephalocraniocutaneous lipomatosis. *Am J Med Genet A* 2007;143A:2963–72.
42. Moog U. Encephalocraniocutaneous lipomatosis. *J Med Genet* 2009;46:721–9.
43. Moog U, Jones MC, Bird LM, et al. Oculocerebrocutaneous syndrome: the brain malformation defines a core phenotype. *J Med Genet* 2005;42:913–21.

44. Laura FS. Epidermal nevus syndrome. *Handb Clin Neurol* 2013;111:349–68.
45. Flores-Sarnat L. Hemimegalencephaly: part 1. Genetic, clinical, and imaging aspects. *J Child Neurol* 2002;17:373–84 [discussion: 84].
46. Sato N, Yagishita A, Oba H, et al. Hemimegalencephaly: a study of abnormalities occurring outside the involved hemisphere. *AJNR Am J Neuroradiol* 2007;28:678–82.
47. Smpokou P, Fox VL, Tan WH. PTEN hamartoma tumour syndrome: early tumour development in children. *Arch Dis Child* 2015;100:34–7.
48. Meltzer CC, Smirniotopoulos JG, Jones RV. The striated cerebellum: an MR imaging sign in Lhermitte-Duclos disease (dysplastic gangliocytoma). *Radiology* 1995;194:699–703.
49. Chen XY, Lu F, Wang YM, et al. PTEN inactivation by germline/somatic c.950_953delTACT mutation in patients with Lhermitte-Duclos disease manifesting progressive phenotypes. *Clin Genet* 2014;86:349–54.
50. Bhargava R, Au Yong KJ, Leonard N. Bannayan-Riley-Ruvalcaba syndrome: MRI neuroimaging features in a series of 7 patients. *AJNR Am J Neuroradiol* 2014;35:402–6.
51. Vanderver A, Tonduti D, Kahn I, et al. Characteristic brain magnetic resonance imaging pattern in patients with macrocephaly and PTEN mutations. *Am J Med Genet A* 2014;164A:627–33.
52. Thomas B, Krishnamoorthy T, Radhakrishnan VV, et al. Advanced MR imaging in Lhermitte-Duclos disease: moving closer to pathology and pathophysiology. *Neuroradiology* 2007;49:733–8.
53. Kulkarnakorn K, Awwad EE, Levy B, et al. MRI in Lhermitte-Duclos disease. *Neurology* 1997;48:725–31.
54. Kimonis VE, Mehta SG, Digiovanna JJ, et al. Radiological features in 82 patients with nevoid basal cell carcinoma (NBCC or Gorlin) syndrome. *Genet Med* 2004;6:495–502.
55. John AM, Schwartz RA. Basal cell nevus syndrome: an update on genetics and treatment. *Br J Dermatol* 2016;174(1):68–76.
56. Sartip K, Kaplan A, Obeid G, et al. Neuroimaging of nevoid basal cell carcinoma syndrome (NBCCS) in children. *Pediatr Radiol* 2013;43:620–7.
57. Choudry Q, Patel HC, Gurusinge NT, et al. Radiation-induced brain tumours in nevoid basal cell carcinoma syndrome: implications for treatment and surveillance. *Childs Nerv Syst* 2007;23:133–6.
58. Amlashi SF, Riffaud L, Brassier G, et al. Nevoid basal cell carcinoma syndrome: relation with desmoplastic medulloblastoma in infancy. A population-based study and review of the literature. *Cancer* 2003;98:618–24.
59. Garre ML, Cama A, Bagnasco F, et al. Medulloblastoma variants: age-dependent occurrence and relation to Gorlin syndrome—a new clinical perspective. *Clin Cancer Res* 2009;15:2463–71.
60. Laugel V. Cockayne syndrome: the expanding clinical and mutational spectrum. *Mech Ageing Dev* 2013;134:161–70.
61. Koob M, Laugel V, Durand M, et al. Neuroimaging in Cockayne syndrome. *AJNR Am J Neuroradiol* 2010;31:1623–30.
62. Faghri S, Tamura D, Kraemer KH, et al. Trichothiodystrophy: a systematic review of 112 published cases characterises a wide spectrum of clinical manifestations. *J Med Genet* 2008;45:609–21.
63. Rapin I. Disorders of nucleotide excision repair. *Handb Clin Neurol* 2013;113:1637–50.
64. Kraemer KH, Patronas NJ, Schiffmann R, et al. Xeroderma pigmentosum, trichothiodystrophy and Cockayne syndrome: a complex genotype-phenotype relationship. *Neuroscience* 2007;145:1388–96.
65. Gripp KW, Lin AE. Costello syndrome: a Ras/mitogen activated protein kinase pathway syndrome (rasopathy) resulting from HRAS germline mutations. *Genet Med* 2012;14:285–92.
66. Gripp KW, Hopkins E, Doyle D, et al. High incidence of progressive postnatal cerebellar enlargement in Costello syndrome: brain overgrowth associated with HRAS mutations as the likely cause of structural brain and spinal cord abnormalities. *Am J Med Genet A* 2010;152A:1161–8.